



ELSEVIER

Journal of Physics and Chemistry of Solids 65 (2004) 139–146

JOURNAL OF
PHYSICS AND CHEMISTRY
OF SOLIDS

www.elsevier.com/locate/jpcs

New carbons with controlled nanoporosity obtained by nanocasting using a SBA-15 mesoporous silica host matrix and different preparation routes

J. Parmentier^{a,*}, S. Saadhallah^b, M. Reda^{a,b}, P. Gibot^a, M. Roux^a, L. Vidal^b,
C. Vix-Guterl^b, J. Patarin^a

^aLaboratoire de Matériaux Minéraux, Ecole Nationale Supérieure de Chimie de Mulhouse, UMR CNRS 7016, Université de Haute Alsace,
3 rue Alfred Werner, Mulhouse Cedex 68093, France

^bInstitut de Chimie des Surfaces et Interfaces–UPR CNRS 9069, 15 rue Jean Starcky, B.P. 2488-Mulhouse Cedex 68057, France

Abstract

An ordered mesoporous silica matrix (SBA-15) was infiltrated with carbon using either a liquid or a gas route with various carbon precursors (sucrose, petroleum pitch and propylene). The resulting SiO₂/C materials were then chemically treated to dissolve selectively the silica matrix and lead to ordered mesoporous carbon replicas. The influence of the precursors on the physico-chemical properties of the SiO₂/C composites and the carbon replicas were studied by X-ray diffraction, nitrogen adsorption measurements, scanning and transmission electron microscopies. It was shown that the content, the route for introducing the carbon into the host matrix, the microporosity and the mesopores order of the carbon replicas are determined by the choice of the precursors. The thermal evolution of the carbon replicas is also studied.

© 2003 Elsevier Ltd. All rights reserved.

Keywords: A. Microporous materials; A. Nanostructures; B. Vapour deposition; D. Microstructure; D. Surface properties

1. Introduction

Nanostructured materials have attracted a large interest for their various potential applications in numerous fields such as energy storage, electrochemistry, adsorption, catalysis, etc. This goal can be achieved if tailored materials with controlled properties can be synthesized. In the particular case of nanoporous carbon materials, micro and mesopores are required to allow the adsorption of large amounts and varieties of chemicals from gases to liquids and the easiness of their diffusion. The classically used activated carbons suffer from an insufficient control of the pore size and arrangement during their preparation processes [1]. Therefore, a new strategy has been proposed based on a host–guest chemistry of porous materials. This concept can briefly be described as follows: a porous material (also named template or mould) is filled with carbon by means of various routes (liquid or gas). The resulting host/carbon materials are then chemically treated to selectively remove the template. A negative carbon replica of the porous structure of the mould is obtained with

well-tailored pore morphology by the porous structure of the host matrix. The synthesis of a very large panel of carbon materials can then be forecast due to the broad variety of available host matrices (lamellar, micro, meso and macroporous). Some applications of these templates are given below.

The carbonization of organic polymer between the layer of clays performed by the group of Kyotani and Tomita led to the formation of unique carbon materials, like ultra-thin graphite film [2]. The authors have noticed that a typical non-graphitized carbon precursor such as polyfurfuryl alcohol can be well graphitized by this method. It means that the structure of the carbon material at the nanometer scale can be influenced and controlled by the size and the shape of the nanopores of the templates. Pillared clays with a higher interlayer spacing (2 nm) were also be used by Bandosz et al. [3].

Microporous templates like zeolites were also tested. Zeolites of structure type FAU (zeolite Y) [4–8], LTL (zeolite L) [4], BEA (zeolite beta) [4], MOR (zeolite Mordenite) [7] and MFI (zeolite silicalite-1) [7] were filled with carbon using various carbon precursors such as acrylonitrile, furfuryl alcohol, organic resin or propylene. Under specific condition, Ma et al. [6] were able to obtained

* Corresponding author. Fax: +33-3-8933-6885.

E-mail address: j.parmentier@univ-mulhouse.fr (J. Parmentier).

pure microporous carbon replica with a surface area as high as $3600 \text{ m}^2/\text{g}$ and with a micropore volume of $1.5 \text{ cm}^3/\text{g}$.

This concept was applied by Ryoo et al. [9] for the synthesis of a carbon replica (named CMK-1) with the use of an ordered mesoporous silica like MCM-48 as template. Since, numerous carbon replicas have been prepared by using different mesoporous templates (SBA-15, HMS, etc.) and carbon precursors. Various carbon-filling techniques were also tested such as the sucrose solution impregnation followed by carbonization [9], or the pyrolytic decomposition of propylene gas [10]. To our knowledge, the study of the characteristics of the carbon replica obtained, for a given mesoporous template, using different carbon precursors and preparation route, has not been investigated.

In the present work, several carbon materials were synthesized by means of two different impregnation routes and three different carbon precursors: the liquid impregnation (with sucrose and pitch) and the gas phase impregnation with propylene. Pitch is an excellent source of graphitizable [11,12] carbon, both readily and cheap since the calcined mesophase formed during the pitch carbonization generates a pre-graphitic structure that can be developed into a graphitic one by a high-temperature treatment. All these infiltrations were performed on the same batch of SBA-15 silica, an ordered mesoporous silica with an one dimensional hexagonal arrangement of mesopores interconnected with micropores. Therefore a 3 D-porosity is present in that host matrix that allows the cohesion of the carbon replica. The present paper deals with the comparison of different carbon-infiltrated silicas (SiO_2/C materials) and their corresponding carbon replicas. The influence of the carbon content was also investigated in order to get a better insight of the mechanisms of the carbon filling within the host matrix regarding to the precursors used. The resulting carbons were characterized using different techniques and their thermal stability (in inert atmosphere) was studied. Moreover, it is worth noting that pitch petroleum was never used as liquid carbon precursor for the infiltration of ordered mesoporous silica materials.

2. Experimental

2.1. Synthesis of the mesoporous silica template: SBA-15

The synthesis of SBA-15 silica was performed using 1 g of Pluronic P123 (BASF), 65 g of H_2O , 9.7 g of 12 M HCl and 2.1 g of tetraethylorthosilicate (TEOS, Fluka, 98%). The mixture of P123/water/hydrochloric acid was stirred vigorously before the TEOS addition. This mixture was aged at 313 K for 24 h followed by a second treatment at 350 K for 24 h. After filtration and washing, the powder is dried at room temperature and heat-treated at 873 K in air for 6 h to remove the organic template before using it as a mould.

2.2. The carbon infiltration processes

The sucrose process is performed as indicated by Ryoo et al. [9] and is not reported in details here. Briefly, a liquid solution of sucrose was mixed with the SBA-15 silica at room temperature in the presence of H_2SO_4 (catalyst) before to be dried and subsequently impregnated with another sucrose solution. The mixture was then heat-treated in vacuum at 1173 K for 3 h. These two liquid-impregnation steps allow a carbon content of 36 wt% to be reached for the SiO_2/C material.

The chemical vapor deposition (CVD) process is based on the pyrolytic decomposition of propylene (2.5 vol% in Argon) at 1023 K on the SBA-15 silica matrix as reported elsewhere [10]. The duration of the deposition allows a control of the carbon content in the final SiO_2/C material. In this study, values in the range 22–52 wt% of carbon into the SiO_2/C have been obtained, compared to the maximal theoretical value of about 63 wt% for the material SBA-15/C used for this study.

For the Pitch process, petroleum pitch named 'Ashland A240' was used as the carbon precursor. A calculated amount of pitch (density 1.24) was mixed with the SBA-15 template in order to fill all its mesoporosity (pore volume $0.95 \text{ cm}^3/\text{g}$). The pitch impregnation was performed by stirring this mixture for 4 h at 575 K (temperature which corresponds to the lowest viscosity of the pitch). The SBA-15/Pitch mixture was cooled down before to be heat-treated in argon up to 1175 K (heating rate: 3 K/min) for the conversion of pitch to carbon. With a pitch having a carbon yield of 45 wt%, a carbon content of about 36 wt% was obtained for the SiO_2/C sample after one-impregnation. A second impregnation was performed on the SiO_2/C sample assuming that all the pitch of the first infiltration was introduced into the porosity. It allows reaching a carbon content of 48 wt%.

All the SBA-15/C samples were then treated with hydrofluoric acid to selectively leach out the silica matrices and recover the carbon replicas [9]. The host silica SBA-15 template as well as the SBA-15/C and the C samples were characterized by different techniques as described below.

2.3. Characterizations

The different materials (SiO_2 moulds, SiO_2/C composites and carbon replicas) were characterized by powder X-ray diffraction (XRD) on a Philips diffractometer ($\text{Cu K}\alpha_1$ radiation ($\lambda = 0.15406 \text{ nm}$)). Nitrogen adsorption/desorption measurements were performed on a Micromeritics ASAP 2010 at 77 K. Prior to the measurements, the samples were outgazed at 473 K overnight. The specific surface area was determined using the BET method in the relative pressure 0.02–0.2 [13]. The pore volume was calculated by considering the volume of nitrogen adsorbed at the value of P/P_0 of 0.95. The mesopore-size distribution was evaluated by the Barrett–Joyner–Halenda method from the desorption

Table 1
Porous characteristics of the SBA-15/C composites

Sample	V_p (cm^3/g)	S_{BET} (m^2/g)	Pore diameter (nm, BJH) [14]
SBA-15 (host matrix)	0.95	800	5.5
SBA-15/ $\text{C}_{\text{CVD-52\%}}$	0.04	25	Non-porous
SBA-15/ $\text{C}_{\text{CVD-36\%}}$	0.31	330	4.5
SBA-15/ $\text{C}_{\text{CVD-22\%}}$	0.46	425	4.0
SBA-15/ $\text{C}_{\text{Sucrose-37\%}}$	0.20	350	4.5
SBA-15/ $\text{C}_{\text{Pitch 2-48\%}}$	0.10	240	Micropores ^a
SBA-15/ $\text{C}_{\text{Pitch 1-36\%}}$	0.06	60	4.4

V_p , total pore volume; S_{BET} , specific surface area.

^a Pore diameter below 2 nm.

branch of the hysteresis loop of the isotherm and using a cylindrical pore model [14].

The High-Resolution Transmission Electron Microscopic (HRTEM) images were performed on a TOPCON EM002B (200 keV, $C_s = 0.4$ mm) electron microscope. The morphology of the initial and final materials was observed on a scanning electron microscope (Philip XL 30).

The materials obtained after the different processes and treatments are referred in the text as SBA-15 for the silica host matrix, SBA-15/ $\text{C}_{X-y\%}$ for the SiO_2/C material obtained

by the infiltration process X ($X = \text{CVD}$, Sucrose or Pitch) with a carbon content of $y\%$. The carbon replicas are named $\text{C}_{X-y\%}$.

3. Results and discussion

3.1. Comparison of the SiO_2/C composites

As shown in Table 1 and as expected, the carbon-filled mesoporous silica samples exhibit a lower pore volume and surface area than the starting SBA-15 template. Nevertheless, differences can be observed depending on the carbon-filling content and the infiltration process used.

The samples having a similar high-carbon content, close to 50 wt% compared to the maximum value of 63 wt%, were obtained using the CVD and Pitch processes (samples SBA-15/ $\text{C}_{\text{CVD-52\%}}$ and SBA-15/ $\text{C}_{\text{Pitch 2-48\%}}$). They both show a similar low pore volume, whereas a strong difference in their specific surface areas can be noticed (25 compared to 240 m^2/g , respectively), suggesting the presence of external carbon in the latter case and/or the formation of micropores within the carbon material.

The SiO_2/C composites containing around 36 wt% of carbon (SBA-15/ $\text{C}_{\text{CVD-36\%}}$, SBA-15/ $\text{C}_{\text{Sucrose-37\%}}$, and SBA-15/ $\text{C}_{\text{Pitch 1-36\%}}$) are nearly half-filled. Therefore, a residual

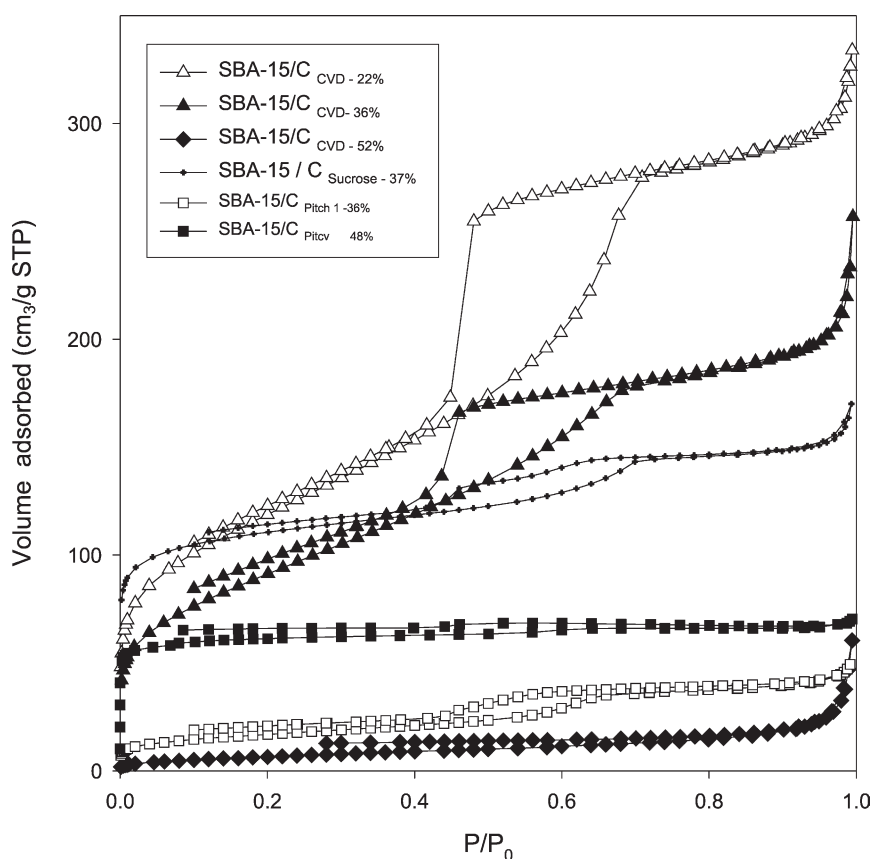


Fig. 1. Nitrogen adsorption/desorption isotherms of the SBA-15/C composite samples.

porosity should be present. A simple calculation based on the pore volume of the silica matrix and the density of carbon and silica gives for the mixed samples, a theoretical pore volume close to $0.44 \text{ cm}^3/\text{g}$, assuming a perfectly homogeneous filling with no pore closure. The isotherms of these three samples represented in Fig. 1 show for all of them, a large step in the range P/P_0 0.4–0.7 characteristic of a large mesopore size distribution with pores of smaller size than the starting SBA-15 sample (steep step in the range P/P_0 0.70–0.75) as reported in Table 1. These features indicate that, whatever the carbon infiltration process used for this carbon content, all the pores are partially filled but not in a homogeneous way (large mesopore size distribution). Moreover, one can notice that at the difference of the SBA-15/ $C_{\text{CVD-36\%}}$ sample, the SBA-15/ $C_{\text{Sucrose-37\%}}$ and SBA-15/ $C_{\text{Pitch 1-36\%}}$ samples display a lower mesopore volume. This observation suggests the presence of a higher volume of closed mesoporosity for the latter samples, especially for the one obtained with the pitch precursor. It is worth noting that the sucrose sample exhibits here a higher

surface area and a higher micropore volume compared to the CVD sample; these could be related to the formation of micropores by the release of volatile species (H_2O , CO , CO_2 ,...) during the conversion of sucrose into carbon.

The decrease in the carbon infiltrated content to a level of 20 wt% leads to an isotherm (Fig. 1) with a typical triangular hysteresis shape (type H2) which is already visible for the CVD sample containing 36 wt% of carbon. This behavior is characteristic of the desorption of nitrogen from ‘bottle shape’ pores. This pore shape can easily be explained by considering that with the CVD process, although propylene penetrates all the mesoporosity, its pyrolytic decomposition at the end takes place preferentially at the entrance of the pores (where the vicinity of the propylene flow allows its renewal) but without pore closure.

The different characteristics of the composite SBA-15/carbon samples can be explained by the filling process. With the CVD process, a homogeneous carbon filling seems to be obtained, the pyrolytic decomposition of

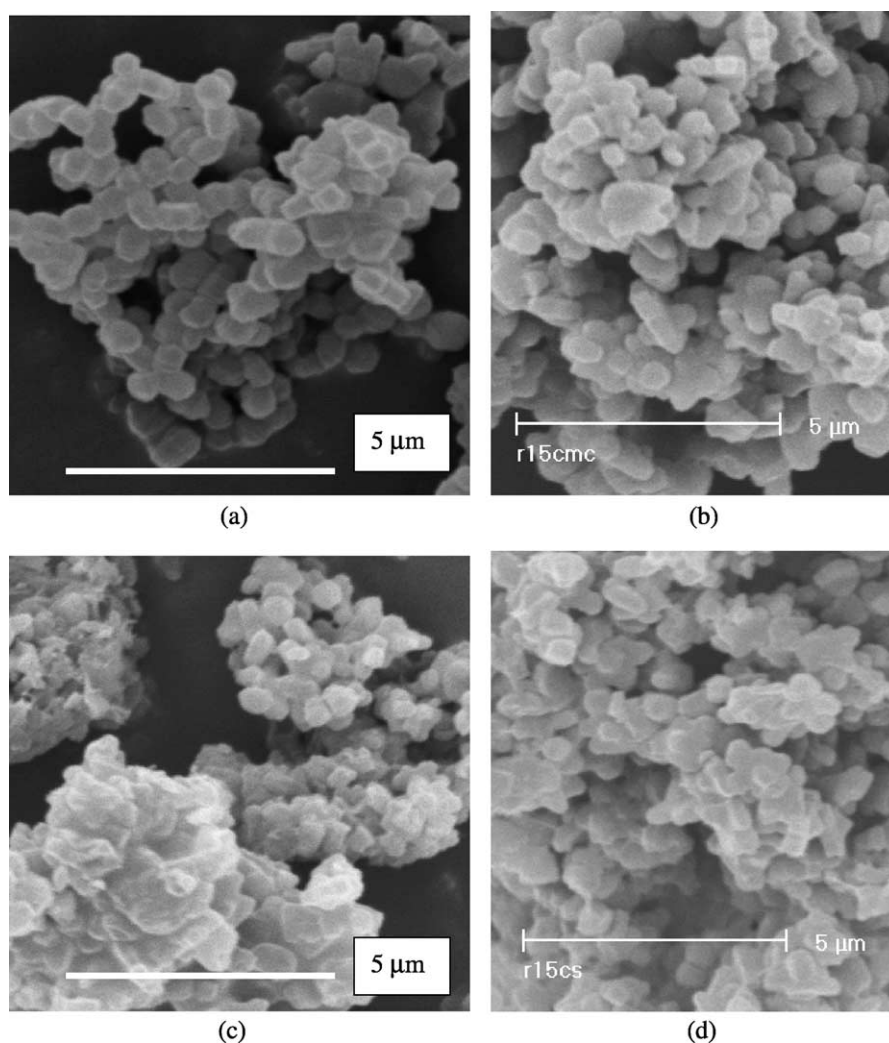


Fig. 2. SEM micrographs of the samples SBA-15 template (a); $C_{\text{CVD-52\%}}$ (b); $C_{\text{Pitch 1-36\%}}$ (c); $C_{\text{Sucrose-36\%}}$ (d).

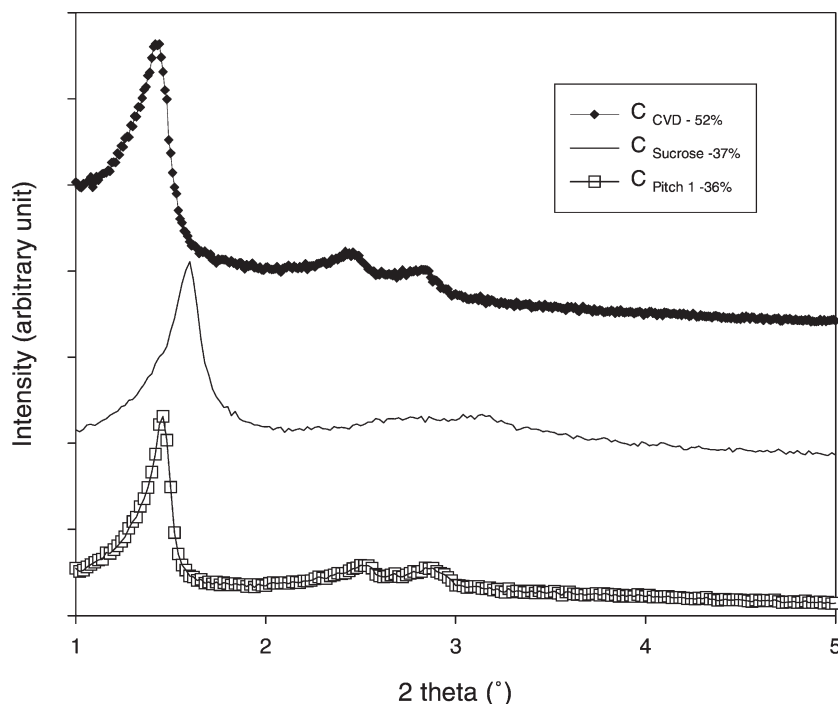


Fig. 3. Powder X-ray patterns of the different carbon replicas (Cu $K_{\alpha 1}$ radiation).

propylene taking place through the entire sample with a carbon deposit at the surface of the pores and at the end preferentially at the aperture of the pores. Nevertheless, a high carbon content can be reached without pore closure at the difference of the liquid processes (Pitch and Sucrose) where a different mechanism takes place. The liquid precursors are in a first step introduced through all the mesoporosity before to be turned into carbon. Therefore, carbon is present through all the silica material but probably with a lower homogeneity than the CVD process. Indeed, with liquid precursors, a phenomenon of mesopore closure seems to be present that hinders a complete and homogeneous carbon-filling, promoting the formation of external carbon especially

for high carbon contents (e.g. Pitch process). These features are verified by SEM for the carbon replicas as described below.

3.2. Study of the SBA-15 carbon replicas

The SEM micrographs of the SBA-15 silica template and its carbon replicas are shown in Fig. 2. One can clearly see, that the particle morphology of the template is conserved for the carbon replicas even when a high-carbon content has been impregnated into the host matrix by the CVD process ($C_{CVD-52\%}$ sample). Nevertheless, with the Pitch process, agglomerates with a less well-defined morphology can be noticed when 36 wt% of

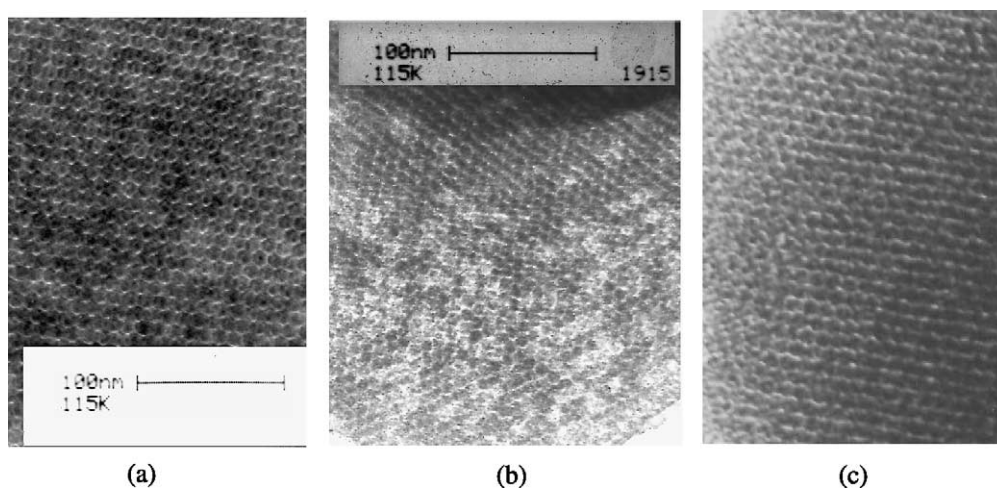


Fig. 4. TEM micrographs of the different carbon replicas: (a) $C_{CVD-52\%}$; (b) $C_{Sucrose-36\%}$ and (c) $C_{Pitch\ 2-48\%}$.

Table 2
Some characteristics of the SBA-15 carbon replicas

Sample	V_p (cm^3/g)	S_{BET} (m^2/g)	A (nm) hexagonal unit-cell parameter ^b
C _{CVD-52%}	0.55	750	10.7
C _{CVD-36%}	1.05	910	10.4
C _{CVD-22%}	1.03	890	10.0
C _{Sucrose-36%}	1.11	1470	9.4
C _{Pitch 1-36%}	0.58	920	10.3
C _{Pitch 2-48%}	0.36	530	9.4

V_p , total pore volume; S_{BET} , specific surface area.

^a For the SBA-15 silica matrix, the hexagonal unit-cell parameter is equal to 11.0 nm.

carbon is introduced into the silica-host matrix (C_{Pitch 1-36%} sample); this observation indicates the presence of external carbon as clearly observed for the C_{Pitch 1-48%} sample (not reported).

Whatever the process used, when the carbon content is higher than 20 wt% [15], one can see on the X-ray patterns (Fig. 3) that the carbon replicas exhibit a long range ordering (hexagonal symmetry) as confirmed by the TEM experiments (Fig. 4). The decrease in the cell parameters (Table 2) can be attributed to a contraction of the silica template during the heat-treatment performed for the carbon infiltration process. The higher temperature used for the Pitch and Sucrose processes (1173 K) compared to the CVD process (1023 K) explains the higher contraction observed for the formers samples.

The pores of the carbon replicas have the shape of the walls of the SBA-15 template. It means that classical gas adsorption/desorption models considering cylindrical pores cannot be applied for these materials. A new model based on rod-aligned slitlike pore [16] was developed for

the MCM-48 carbon replica but to our knowledge, no new model was proposed for the SBA-15 replica. Therefore, the interpretations of the carbon isotherms (Fig. 5) are at the present time still unclear. The characteristics of these isotherms (pore volume V_p and specific surface area (S_{BET})) are reported in Table 2.

The pore volume differs depending on the amount of total carbon introduced into the silica matrix and the proportion of external carbon. As mentioned above, with the CVD process, a homogeneous carbon filling is obtained and for a high carbon content the carbon replica (C_{CVD-52%} sample) is characterized by a pore volume close to $0.55 \text{ cm}^3/\text{g}$, whereas when the amount of carbon infiltrated into the host matrix decreases, more void remains leading to a carbon replica with a higher pore volume.

For the pitch process, the sample with a high carbon content (C_{Pitch 2-48%}) exhibits a lower pore volume compared to the CVD sample in relation to its high external content of carbon as assumed above. Moreover, this type of carbon seems to be poorly porous as suggested by the low surface area measured. For this process, a decrease in the carbon content allows a better control of the carbon filling and therefore an increase in the pore volume and surface area (see Table 2, sample C_{Pitch 1-36%}). For similar carbon contents, the CVD and Sucrose processes lead probably to a lower proportion of external carbon as proved by the higher pore volume obtained. It is worth noting that with the sucrose process, an additional microporosity is created during the carbonization step by the release of volatile species as shown by the high pore volume and surface area of the carbon replica.

The thermal stability of these carbon replicas and their ability to graphitize were studied by XRD. One can see on the corresponding patterns recorded at low angles

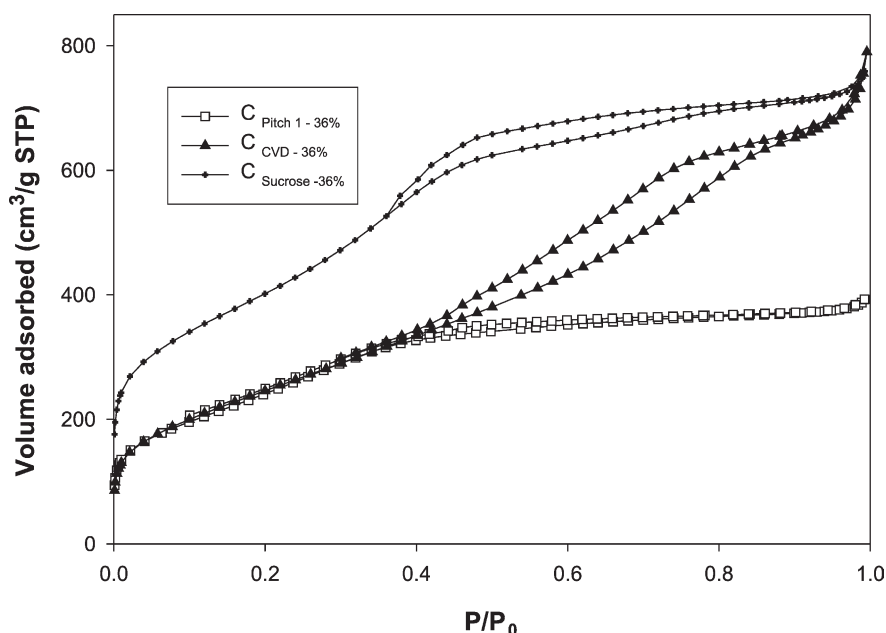


Fig. 5. Nitrogen adsorption/desorption isotherms of the carbon replicas C_{CVD-36%}, C_{Pitch 1-36%}, C_{Sucrose-36%}.

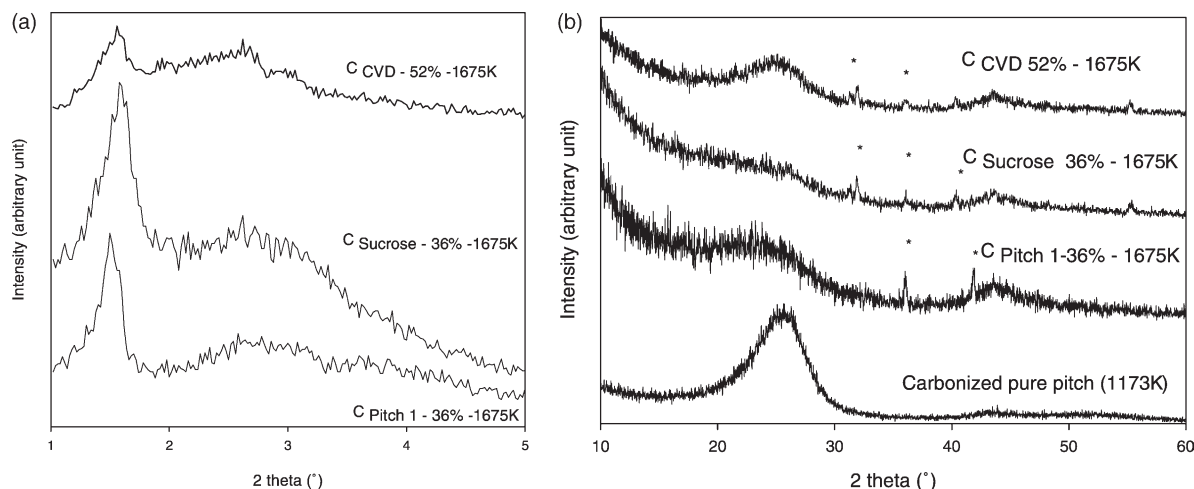


Fig. 6. Powder XRD patterns of the carbon replicas heat-treated at 1675 K (Cu $K_{\alpha 1}$): (a) low angles; (b) high angles. For comparison, the XRD pattern of a pure carbonized pitch sample is also represented (* : impurities).

(Fig. 6(a)) that the relative intensity of the more intense correlation peaks have decreased and that the two distinct peaks in the 2θ range of $2\text{--}3^\circ$ have disappeared after the heat-treatment at 1675 K. It means that the heat-treatment alters slightly the long-range order of the carbon replicas as confirmed by the TEM observations which pointed out the existence of microdomains having different orientations within the particles (not reported). Nevertheless, the latter technique has shown that the local order at the mesoscopic scale is preserved. XRD patterns recorded at 2θ angles above 10° are characteristic of a poorly organized carbon structure at the atomic scale (Fig. 6(b)). The presence of a broad peak around 25° (2θ), observed only for the $C_{\text{CVD-52\%-1675 K}}$ and $C_{\text{Pitch-36\%-1675 K}}$ samples, can be ascribed to the turbostratic carbon structure. This feature is consistent with the fact that the carbon materials obtained from pitch carbonization or pyrolytic decomposition of propylene are well known to lead to graphitizable carbons contrary to the one prepared by infiltration of sucrose. For comparison, the XRD pattern of a pure carbonized pitch sample calcined at 1173 K is also reported in Fig. 6(b). Although, a higher carbonization temperature is used, it is worth noting that the intensity of this peak for the $C_{\text{Pitch-36\%-1675 K}}$ sample is lower than the one observed for the pure carbonized pitch sample, suggesting that the pitch carbonization taking place in a mesoporous confined media may be lead to a carbon material with different characteristics.

4. Conclusion

The comparison of the SiO_2/C materials and the corresponding carbon replicas has shown that the mechanism of the carbon infiltration differs according to the carbon precursor used. Although a given silica template allows a control of the pore morphology of

the carbon replica (the pore has the shape of the walls of the host matrix), the nature of the carbon precursor influences also directly the characteristics of the porous structure of the material to which it is converted. Indeed, for a mesoporous template, each carbon precursor has its own maximal carbon content per infiltration step; then the resulting carbons differ as regards porosity (presence of an additional microporosity with sucrose), compositions, nanometric scale organization (graphitization). These model carbon materials, with various controlled characteristics, could also contribute to determine the optimal properties of some of their potential applications.

Acknowledgements

The French Minister of Research and the CNRS are also gratefully acknowledged for their financial supports through the ‘Nanosciences-Nanotechnologies’ and ‘Materials’ programs.

References

- [1] T. Kyotani, Carbon 38 (2000) 269–286.
- [2] (a) T. Kyotani, N. Sonobe, A. Tomita, Nature 331 (1988) 331–333. (b) N. Sonobe, T. Kyotani, A. Tomita, Carbon 29 (1991) 61–67. (c) T. Kyotani, T. Mori, A. Tomita, Chem. Mater. 6 (1994) 2138–2142.
- [3] (a) T. Bandoz, K. Putyera, J. Jagiello, J.A. Schwarz, Carbon 32 (1994) 659–664. (b) T. Bandoz, J. Jagiello, K. Putyera, J.A. Schwarz, Langmuir 11 (1995) 3964–3969. (c) T. Bandoz, J. Jagiello, K. Putyera, J.A. Schwarz, Chem. Mater. 8 (1996) 2023–2029.
- [4] S.A. Johnson, E.S. Brigham, P.J. Olliver, T.E. Mallouk, Chem. Mater. 11 (1997) 2448–2458.
- [5] J.R. Odriguez-Mirasol, T. Cordero, L.R. Radovic, J.J. Rodriguez, Chem. Mater. 10 (1998) 550–558.
- [6] Z. Ma, T. Kyotani, A. Tomita, Carbon 40 (2002) 2367–2374.
- [7] P. Enzel, T. Bein, Chem. Mater. 4 (1992) 819–824.

- [8] T. Kyotani, T. Nagai, S. Inoue, A. Tomita, *Chem. Mater.* 9 (1997) 609–615.
- [9] R. Ryoo, S.H. Joo, S. Jun, *J. Phys. Chem. B* 103 (1999) 7743.
- [10] J. Parmentier, J. Patarin, J. Dentzer, C. Vix-Guterl, *Ceram. Int.* 28 (2002) 1–7.
- [11] I. Mochida, Y. Korai, C. Ku, F. Watanabe, Y. Sakai, *Carbon* 38 (2000) 305.
- [12] B. Rand, *Design and Control of Structure of Advanced Carbon Materials for Enhanced Performance*, Kluwer, The Netherlands, 2001.
- [13] S. Brunauer, P.H. Emmett, E. Teller, *J. Am. Chem. Soc.* 60 (1938) 309–319.
- [14] P. Barrett, L.G. Joyner, P. Halenda, *J. Am. Chem. Soc.* 73 (1951) 373–385.
- [15] F. Ehrburger-Dolle, I. Morfin, E. Geissler, F. Bley, F. Livet, C. Vix-Guterl, S. Saadallah, J. Parmentier, M. Reda, J. Patarin, M. Iliescu, J. Werckmann, *Langmuir* 19 (2003) 4303–4308.
- [16] T. Ohkubo, J. Miyawaki, K. Kaneko, R. Ryoo, N.A. Seaton, *J. Phys. Chem. B* 106 (2002) 6523–6528.